www.ijbar.org
ISSN 2249-3352 (P) 2278-0505 (E)
Cosmos Impact Factor-5.86

Enhancing Image Resolution Through Anchored Deep Learning Models

Mr.Kyasanipalli Sagar Sanjeev
Assistant Professor, Department of ECE,
Malla Reddy College of Engineering for Women.,
Maisammaguda., Medchal., TS, India

Abstract

Analyzing photos and videos in real time is a challenging problem in smart monitoring applications. Many applications have to choose between frame rate and sharpness due to network limits. Consequently, many security systems now include super-resolution photography as a basic feature. Present image super-resolution methods perform better when used with images taken prior to their full potential. Present photo super-resolution methods based on deep learning seldom take older pictures into account. Consequently, how to maximize the use of image prior is one of the unanswered concerns about deep-network-based single-image super-resolution methods. To close the gap between deep-learning-based single-image super-resolution approaches and the more traditional sparse-representation-based methods, we apply transfer learning to make sure that the deep network we propose takes the previous picture into consideration. Using a deep learning-based single-image super-resolution method still leaves the question of how to stop neurons from sacrificing certain aspects of the image. Picture patches are attached to lexicon atoms in this work for the purpose of class sorting. The network performs better when retrieving high-frequency data as each neuron is trained on visually similar locations.

1 Introduction

Recent years have seen a surge in interest in studying "big data" [4, 7], "the cloud," and "artificial intelligence." The use of deep learning for AI has graduated from the lab and into the uses, particularly in the areas of computer vision, natural language processing, and voice recognition [8, 21]. Sensors [5, 6], like webcams in computer vision, are necessary for interaction with the actual world in these uses. Unfortunately, these gadgets have a very low data transfer rate. The capacity of a USB 2.0 port, for instance, is around 480 Mbps. With a frame rate of 100 hertz and an image of 1920 by 1080, the required bandwidth is approximately 5 Gbps.In additions; there are fast-paced uses that demand a frame rate of more than 100 hertz. As a result, many uses for real-time media require techniques like super-resolution and frame-rate up-conversion. Super-resolution in a monitoring setting is depicted in Figure 1.

This means that even though the instruments have a low-bandwidth link, the pictures sent to the computer can be processed quickly. In addition, the timing issue is complicated in various transmission settings due to the large capacity [26-28]. The low-resolution (LR) raw pictures are mapped to the high-resolution (HR) equivalent using image super-resolution (SR) technology. To date, it has long-studied, but only recently popularized by the latest ultra-high-definition (3840 2048) televisions. Unfortunately, most videos can't be watched in UHD. To create UHD material from FHD (1920 x 1080) or lesser images, SR techniques are required [16]. Single-image SR and multiple-image SR methods categorize pictures for SR based on the number of LR images used as input. In this work, we zero in on single-image SR, which seeks to restore a high-resolution picture from a single input.

www.ijbar.org
ISSN 2249-3352 (P) 2278-0505 (E)
Cosmos Impact Factor-5.86

Fig. 1 An example of super-resolution

Using just one picture of poor quality. For the sake of organization, we classify single-image SR techniques into two broad categories: those that do not rely on deep learning and those that do. Those built on deep learning. While deep learning-based methods always learn a basic end-to-end correspondence between the LR and HR images, most single-image SR methods that don't rely on it either attempt to discover new types of image prior or suggest a new way to use these existing image prior. Image previous, such as local smoothing, nonlocal self-similarity, and scarcity, has been shown to play a significant part in image SR by traditional non-deep-learning-based SR techniques. Small image regions from both the low-resolution and high-resolution images are thought to create low-dimensional nonlinear manifolds with the same local shape in neighbor embedding (NE) methods.

Using the locally linear embedding (LLE) technique of manifold learning, Chang et al. [3] suggested an SR approach based on this concept. Image scarcity is widely used in the literature of single-image SR, alongside the local linear prior. Assuming that low-frequency image patches have the same sparse representation as the equivalent high-frequency image patches, Yang et al. [35] suggested the first sparse-representation-based single-image SR technique. Based on these findings, Zeyde et al. [37] suggested a more effective vocabulary learning technique that reduces training time significantly for both low- and high-resolution patches. The regularization term, which can be any type of image precondition, has been extensively investigated, including local flattening and nonlocal self similarity. In the single-image SR techniques that rely on restoration constraints. Some older approaches seek to discover a more condensed version of the well-known image prior or a more effective way to use this image prior for enhancing image SR performance, rather than exploring the new image prior. Using anchored neighborhood regression (ANR), Timofte et al. [30] suggest a method for single-image SR. A low-resolution patch's neighborhood embedding can be anchored to the closest element in the lexicon, and the associated embedding matrix can be recomputed. They go on to suggest an enhanced form of ANR in [31], which takes the finest features of both ANR and SF and merges them.

Zhang et al. [38] suggest a dual lexicon for iteratively learning residual that makes greater use of the picture sparse prior. The deep learning approach has been widely discussed recently, and it has been effectively implemented in a wide variety of low- and high-level computer vision issues. There have also been some investigations into picture SR techniques that use deep learning. Dong et al. [10, 11] suggested SRCNN as the first study of its kind in deep learning-based SR. They proved that an end-to-end translation from low-resolution to high-resolution images can be learned by a convolutional neural network (CNN). It does not necessitate the use of designed characteristics, as is the case with more conventional, non-deep learning-based approaches. Following that, they improved the repair of JPEG compressed images by expanding on this work [9]. More recently, they suggested an enhanced variant of SRCNN (FSRCNN) [12] by considering the 1 1 convolution to decrease network weights. Some works attempt to learn the image residual, in contrast to [9–12] which use the original, unaltered picture as ground truth for training. In order to hasten the convergence rate, Kim et al. [17] suggested a very deep network for learning residual. The low-resolution input picture must be upscale to the high-resolution space using a single filter, typically bicubic interpolation, before rebuilding using any of the aforementioned techniques (with the exception of FSRCNN).
To reduce processing overhead, Shi et al. [29] suggested up scaling the final LR feature maps into the HR output by introducing an efficient sub-pixel convolution layer that trains an array of up scaling filters. Both single-image [15, 20, 34] and video [2, 14] SR techniques have seen numerous recent proposals built on deep learning.

2 Related works

www.ijbar.org
ISSN 2249-3352 (P) 2278-0505 (E)
Cosmos Impact Factor-5.86

Since the anchored neighborhood regression serves as the basis for our suggested method, we are able to fully exploit the benefits of both sparse representation methods and the ones built on deep learning, we quickly go over them.

Sparse representation approaches

Low density of resemblance Reduce the number of factors that are not negative to best reflect the signal's essential properties. Sparse representation discovery for patch xi. Sparse coding is the process of encoding a vector I in terms of an already-established, over-complete lexicon D. As can be seen, the null space of D adds extra degrees of freedom in the option of me, which can be used to increase its compressibility as a result of its over-completeness. Sparse coding can be written as follows, yielding the sparse representation:

$$\alpha_i = \arg\min_{\alpha_i} \|x_i - D\alpha_i\|_2^2 \quad s.t. \ \|\alpha_i\|_0 < L \qquad (1)$$

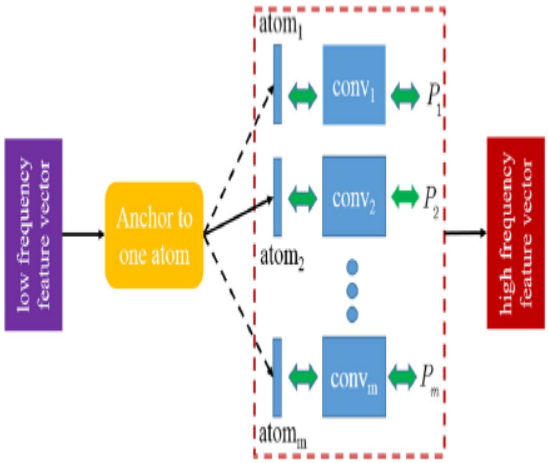

The fixed neighborhood convolution layer is depicted in Fig. 2. Each low-frequency feature vector you feed in will be tied to a lexicon element that will trigger the convolution layer that best fits its characteristics. The low-frequency feature vector is then mapped to the high-resolution space by the enabled convolution layer. The green arrow with two heads indicates that one lexicon atom and one projection matrix are linked to each convolution layer. Although approximating this issue is difficult, many different methods exist [22]. In this article, we utilize the straightforward and effective orthogonal matching pursuit (OMP) [32] method to address this issue. Dictionary learning is the other major issue with limited representation. It can be stated generally as:

$$D, \{\alpha_i\} = \arg\min_{D,\{\alpha_i\}} \sum_k \|x_i - D\alpha_i\|_2^2 \quad s.t. \ \|\alpha_i\|_0 < L \ \forall i \qquad (2)$$

Where I is a vector that represents xi in a fragmented form.

In the past year, numerous strategies for memorizing dictionaries have been suggested. One of the most popular dictionaries K-SVD [18] is one of the most effective and efficient vocabulary learning techniques currently available, outperforming many other state-of-the-art approaches. The SR technique based on sparse representations implies that low-resolution areas have the same sparse representation as their high-resolution counterparts. Therefore, limited vocabularies for both low- and high-resolution picture regions must be learned simultaneously. The combined vocabulary learning can be stated in the following way, given a collection of training picture patch pairs Xh and Xl:

$$\arg\min_{D_l,D_h,\alpha} \frac{1}{N}\|X_h - D_h\alpha\|_2^2 + \frac{1}{M}\|X_l - D_l\alpha\|_2^2 + \lambda\left(\frac{1}{N}+\frac{1}{M}\right)\|\alpha\|_0 \qquad (3)$$

Where N and M denote the high- and low-resolution patches and their dimensions, and is the coefficient vector indicating scarcity; Xh and XL are the high- and low-resolution patches, respectively. Timofte et al. [30] suggested anchored neighborhood regression for rapid single image SR to reduce computation time. They used a subset of the dictionary elements to symbolize each patch and loosened the L0 norm constraint to L2. Then the criterion for success will be to

$$\alpha_i = \arg\min_{\alpha_i} \|x_i - D_l\alpha_i\|_2^2 + \lambda\|\alpha_i\|_2 \qquad (4)$$

The L2 norm provides a closed answer by transforming the issue into ridge regression. It is

www.ijbar.org
ISSN 2249-3352 (P) 2278-0505 (E)
Cosmos Impact Factor-5.86

possible to create a high-resolution output from a low-frequency input patch yi. Area as

$$x_i = D_h\left(D_l^T D_l + \lambda I\right)^{-1} D_l^T y_i = P_i y_i \quad (5)$$

Where Pi is the projection matrix that has been saved for the element Dil in the lexicon. In conclusion, ANR calculates the forecast in an inaccessible during training; the system generates a projection matrix Pi for each dictionary atom, maps each patch to its most comparable dictionary atom, and outputs a high-frequency detail patch. Timofte et al. [31] suggest A+, a variation of ANR that merges the finest features of ANR and SF.For additional information on ANR and A+, please see [30, 31].

Deep learning approaches

Traditionally, deep-learning-based image SR methods have learned an end-to-end mapping that immediately converts the low-resolution input picture into a high-resolution target. One with a lot of detail. SRCNN [10], a basic three-layer network, was the first of its kind. In particular, the original image's contiguous patches are extracted in the first layer, and each patch is then represented as a high-dimensional vector in the second. Next, a non-linear mapping layer is applied, which converts each high-dimensional vector from the previous layer into a new high-dimensional vector that represents a high-resolution patch mentally. In the end, the rebuilding layer compiles all the patch-wise depictions into a single result. Kim et al. [17], motivated by the results of other cutting-edge works, suggested expanding the network's depth to increase its receptive field for predicting picture features and employing the residual learning technique to speed up convergence. Wang et al. [34] created a network that functions similarly to the classic sparse-representation-based SR approach. The exact sparse depiction, however, requires numerous levels, and the same network structure is employed by all the picture segments. There are a plethora of alternative picture SR approaches that rely on deep learning.

3 Motivations and contributions

Single-image SR techniques that don't rely on deep learning typically seek out novel forms of image prior or suggest novel applications of existing image prior. All These studies showed that utilizing image priors to their maximum potential can boost image SR results. Few studies have looked into how to make use of the picture previous in deep learning-based techniques. As a result, it motivates us to research how to incorporate picture prior into a deep-learning-based approach. Fortunately, the objective function with a sparse prior restriction has a closed solution, as demonstrated by the work of Timofte et al. [30, 31]. What's more, a convolution layer can readily perform the matrix multiplication. Because of this, it makes perfect sense to use the weights from the offline-trained projection matrix in a convolution layer. These earlier deep-learning-based techniques use neurons that operate on the entire input feature map. They have to settle for subpar visual material. Timofte et al.'s [30, 31] ANR and A+ motivate us to attach distinct image patches to distinct lexicon atoms; this easily divides the patches into multiple groups, allowing each neuron to focus on image patches that are akin to its own.

Instead of training the matrix online with a small number of patches and an image prior, as has been done in earlier works, we suggest in this article to transmit its weights. Limitation, on the convolution layer's weights. As a consequence, our network naturally incorporates the picture previous into its calculations. Like ANR and A+, we first apply the low-frequency input vector to forecast the high-frequency information by anchoring it to one of the lexicon elements and then using the appropriate convolution layer. For this reason, we train our network so that each neuron operates on the same classes of picture segments. In a nutshell, the primary benefits of this study lie in three areas:

We link our deep-learning-based single-image SR technique to the standard sparse representation approach. To combine the best of worlds, the deep-learning-based strategy, which has powerful end-to-end optimization ability, and the more conventional method, which has a good ability of using picture previous knowledge, transfer learning technology has been used. We suggest a deep network that is linked to a community for use in single-image SR. Our suggested SR network's neurons, unlike those in prior deep-learning-based techniques, prioritize acquiring local image information over accommodating a wide variety of image contents. Traditional fixed neighborhood regression techniques are examples of local optimization, while the suggested network optimizes the entire process from beginning to finish.

www.ijbar.org
ISSN 2249-3352 (P) 2278-0505 (E)
Cosmos Impact Factor-5.86

We provide extensive tests to show that our novel single-image SR technique works well.

4 Proposed methods

Our suggested method is an end-to-end projection that utilizes the low-resolution picture as input and out-performs prior deep-learning-based single-image SR methods. Produces the high-resolution version immediately. We use a fixed neighborhood convolution layer to prevent neurons from compromising into various image contents and a sparse prior constraint convolution layer to account for the images sparse prior. As a result, we begin by introducing two convolution layers, one with a sparse prior restriction and another with an attached neighborhood, both of which are specifically tailored to the issues we're interested in solving. We conclude by unveiling our improved network architecture for single-image SR.

Sparse prior constraint layer

For the L2 norm sparse constraint objective function, where the projection matrix is recomputed offline by a series of low-and-slow iterations, the answer xi = Piyi is shown to be very near. Set of high-image patches. It is possible to anticipate finer picture details using a convolution layer by treating each entry of the projection matrix Pi as a filter. In this case, let's say yi is an n1-dimensional vector, xi is an m1-dimensional vector, and Pi is a mn-dimensional matrix. Then, the dimension of each convolution is 11n, where 11 is the geographic area and n is the number of feature maps. There are m convolutions of dimension 11n because the projection matrix Pi has m rows. It's important to observe that each filter is completely unbiased so that they can all serve as adequate representations of the matrix multiplying operation.

Anchored neighborhood layer

In the offline training procedure, the ANR and A+ first locate the areas, and then independently compute a projection matrix Pi for each dictionary element Di. As a result, it only needs to keep the projection matrix Pi and attach the input patch feature yi to its closest neighbor atom Di to produce a map from Di to HR space. In this article, we employ a network to simulate this procedure, as networks possess a property that improves our method's efficiency. Figure 2 depicts the structure of an attached neighborhood convolution layer. We apply the same approach as A+, which accounts for the image sparse previous, to determine the projection matrix Pi for each dictionary element Di. Once all projection matrices have been trained, we use the aforementioned technique to move them to new convolution layers. In other words, the fixed neighborhood layer is composed of sparse prior constraint convolution layers, each of which is dedicated to a single particle. It is important to remember that all of these sub-convolution levels can be performed in simultaneously. The fixed neighborhood layer assigns a single dictionary element to each low-frequency feature vector in the input, which then triggers the appropriate sub-convolution layer. The enabled convolution layer then performs the standard matrix multiplication by mapping the low-frequency feature vector to the high-resolution space.

Proposed network structure

Figure 3 depicts the suggested network architecture. A basic breakdown would be as follows: feature extraction layer, fixed neighborhood convolution layer, a sub network of deep integration and the combo layer. In Fig. 3, we've color-coded the matching components to make it easier to spot them. Taking out features. The characteristics employed to depict the picture segments have a significant impact on performance, as evidenced by the ANR and A+. The fix itself is the simplest component to employ. However, this does not improve the feature's generalizability. One characteristic with a lot of overlap is the patch's first- and second-order variant [3, 35]. In this work, we isolate the picture feature using a convolution layer with n1 filters of size 3s 3s 1, where s is the magnifying factor. As a consequence, the feature vector at the end is n1 by 1. Meanwhile, LR patches are extracted via "one-hot" convolution, wherein a single filter is responsible for extracting a single pixel from the receptive field. One-hot convolution uses a filter size of 3s 3s 1. Convolution anchored to a community. Section 4.2 provides an in-depth explanation of this stratum. It's a quick and precise way to capture images in advance. Picture specifics to be predicted and local image regions to be worked on by the neurons to prevent compromising on various image contents. Keep in mind that our 1024-atom lexicon was used in this

www.ijbar.org
ISSN 2249-3352 (P) 2278-0505 (E)
Cosmos Impact Factor-5.86

exercise. This fixed neighborhood layer contains 1024 parallel sparse prior constraint layers.

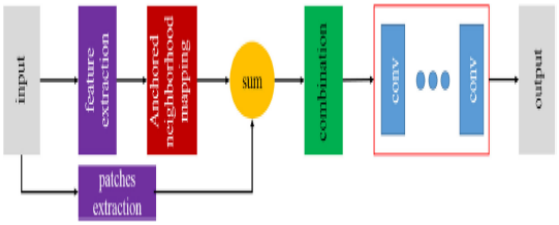

The embedded neighborhood deep network structure is depicted in Fig. 3 and is suggested for use in single-image SR. To forecast the high-frequency features, it first employs a convolution layer to retrieve the low-frequency ones, and then a fixed neighborhood convolution layer. Cascaded convolution layers are used to merge patches of local resemblance and improve picture features after the high-frequency patches have been combined. Picture prediction, uses a single filter with dimensions f f d.

One possible formulation is

$$F_i(y) = \max(0, w_i * y + b_i), i \in \{1, m-1\} \quad (6)$$

$$F_m(y) = w_m * F_{m-1}(y) + b_m \quad (7)$$

Training

Here, we lay out the goal we want to reduce in order to determine the best values for our model's characteristics. In line with other deep-learning-based approaches to picture repair, the network's cost function is the mean square error. Our objective is to learn a transformation f from low-resolution images as input to an estimate of the matching high-resolution picture as output, denoted by y = f (x). Low-resolution counterparts to a given collection of high-resolution picture samples (yi, i = 1... N) Are generated (in reality, they are upscale to the original dimensions via bicubic interpolation). Then, the goal of minimization is written as

$$\min_{\theta} \frac{1}{2N} \sum_{i=1}^{N} \left\| f(x_i; \theta) - y_i \right\|_F^2 \quad (8)$$

In which f (xi ;) is the predicted high-resolution picture with regard to the low-resolution image xi, and is the training value for the network. We employ an adaptable instant estimation (Adam) [18] to fine-tune every variable in the network.

5 Experimental results and discussion

Here, we conduct an in-depth analysis of our method's efficiency across multiple test data sets. We start by talking about the samples we used to train and evaluate our algorithm. After that, some Instructional specifics are provided. We conclude by comparing five modern techniques quantitatively and qualitatively. In this paper, we introduce ANNet, an attached neighborhood deep network.

Implementation details

Test and training datasets. It is common knowledge that a high-quality training sample is crucial to the success of any learning-based picture repair technique. Extensive preparation the literature contains datasets for your perusal. Both SRCNN [10, 11] and VDSR [17] use datasets with 91 and 291 images, respectively. In this study, we primarily use the General-100 dataset, which consists of 100 bmp file pictures, in accordance with FSRCNN [12]. (With no compression). In order to further investigate the effect that varying training databases have on performance, we also create our own. Table 1 we compare our suggested approach to others using Set5 [1] and various filter sizes by calculating the average PSNR (dB) and SSIM.

Filter size	3	5	7	9
3	32.68/0.9106	32.70/0.9108	32.72/0.9104	32.72/0.9104
5	32.80/0.9117	32.74/0.9106	32.79/0.9110	32.78/0.9113
7	32.75/0.9105	32.78/0.9111	32.78/0.9111	32.81/0.9113
9	32.78/0.9108	32.78/0.9109	32.80/0.9114	32.82/0.9114

All models are trained on the General-100 dataset

Collection that includes 260 photos in bmp file. To get ready for training, we use data supplementation (rotation or reverse) and fix the patch size to 45 by 45. Based on the FSRCNN and SRCNN, we use the widely-used Set5 [1] (5 images), Set14 [37] (14 images), and BSD200 [23] (200 images) datasets to

www.ijbar.org
ISSN 2249-3352 (P) 2278-0505 (E)
Cosmos Impact Factor-5.86

conduct our tests. Keep in mind that the test pictures and the data used to train the system are completely distinct. Method for training. We employ the procedure outlined by The et al. [13] to initialize weights. For networks with corrected linear units, this is a mathematically valid method. (ReLu). Adam's other hyper-parameters include a first moment estimate exponential decay rate of 0.90 and a second moment estimate exponential decay rate of 0.999. All of our trials are trained with a group size of 64 and 30 epochs of training. In the first 10 epochs, the learning rate is 0.0001, in epochs 11–20 it's 0.00001, and in the last 10 epochs it's 0.000001.
We use the MatConvNet software [33] to put our model into action.

Investigation of different settings

We create a series of sanity checks to ensure the integrity of our embedded neighborhood deep network. The effects of various parameters, including filter height, network depth, the training data collection, etc. Given that the projection matrix is learned offline and thus locks in the parameters of the embedded neighborhood layer, our focus is on experimenting with various configurations of the deep integration sub network.

Table 2 shows how our suggested approach compares to others at varying levels on Set5 [1] in terms of average PSNR (dB) and SSIM.

Image	2 layers	3 layers	4 layers
Baby	35.25/0.9240	35.26/0.9244	35.33/0.9250
Bird	35.52/0.9565	35.78/0.9584	35.97/0.9596
Butterfly	27.92/0.9166	28.39/0.9235	28.44/0.9249
Head	33.71/0.8254	33.77/0.8279	33.78/0.8286
Woman	31.51/0.9315	31.67/0.9338	31.70/0.9344
Avg.	32.78/0.9108	32.97/0.9136	33.05/0.9145

All models are trained on the General-100 dataset

Table 3 Comparison of our proposed ANNet trained with different datasets

Image	Baby	Bird	Butterfly	Head	Woman	Avg.
Small dataset	38.68/0.9656	41.07/0.9866	32.11/0.9648	35.74/0.8870	35.42/0.9702	36.56/0.9548
Big dataset	38.54/0.9655	41.28/0.9870	32.99/0.9685	35.75/0.8867	35.56/35.42	36.83/0.9557

We begin by looking into how filter size affects speed. The deep integration sub network used in these tests consists of only two convolution layers. In general, Table 1 displays the PSNR and SSIM results from the Set5 dataset used in these studies. The filter size of the first convolution layer of the deep integration sub network is shown in the first column, and the filter size of the second convolution layer is shown in the first row. Since our network's first and second levels of the deep integration sub network have spatial sizes of 3 by 3 and 5 by 5, respectively, the average PSNR and SSIM values can be found in the second and third rows, respectively. The square filter allows us to reduce them to a single value. As can be seen in Table 1, filter efficacy improves with increasing filter size. That's because its bigger receptive field allows it to gather more relevant data for predicting picture features.
Finally, we explore how the training sample itself affects efficiency. Generally speaking, we use General-100 as the training dataset and FSRCNN as our guide. We create our own training dataset consisting of 260 pictures in bmp file to further examine the effect of training dataset on performance. The PSNR and SSIM values for Set5 of our suggested ANNet after training with various datasets are displayed in Table 3. Compared to our newly formed dataset, which includes 260 pictures, the smaller dataset (representing General-100) is relatively tiny. Our network trained with a bigger dataset outperforms one trained with a smaller dataset by about 0.27 dB on this test dataset, on average. That's why having access to a sizable training sample can do wonders for a network's efficiency.

Comparisons with state-of-the-art methods

Four state-of-the-art learning-based single-image SR techniques, including A+ [31], SRF [25], SRCNN [10, 11], and SCN [34], are compared to our ANNet. A+ and SRF and SRCNN are the two most advanced

www.ijbar.org
ISSN 2249-3352 (P) 2278-0505 (E)
Cosmos Impact Factor-5.86

non-deep learning-based techniques, while SCN and SRCNN are the most advanced deep learning-based methods.

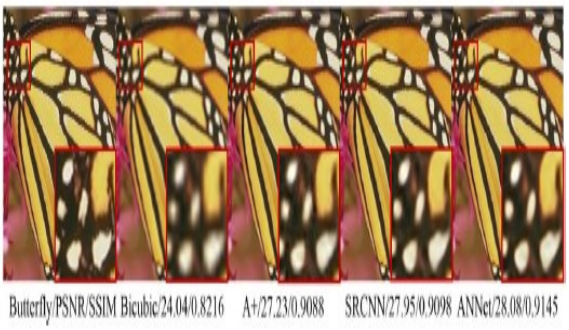

Figure 4 shows a visual contrast of two common deep-learning-based single-images SR techniques using the butterfly picture from Set5 [1] and an up scaling factor of 3. The numeric findings are summarized in Table 4. Testing across multiple data sets. The other four techniques produce the same outcomes as those presented at FSRCNN [12]. Our Annett's experiment-running parameters include a deep integration sub network with two levels using filter sizes of 5 and 3, respectively. It is not learned on our own massive dataset, but rather on the publicly available, much smaller General-100 dataset. As can be seen in Table 4, our suggested ANNet works better than A+, SRF, and SRCNN. Our ANNet outperforms Bicubic, SRCNN, A+, and SRF on this setup and test dataset by an average of 1.97, 0.38, 0.24, and 0.1 dB, respectively. The average PSNR disparity between our ANNet and SCN is only 0.04 dB, so the two networks are similar. In addition, SCN requires a number of chain processes for optimal efficiency. As we saw above, we can improve efficiency by increasing network depth or by using a bigger training sample. In addition to the quantitative data presented in Figs. Figure 4 displays a graphic contrast of the three different up scaling factors used for the butterfly picture in Set5 when using single-image SR. Figure 5 shows an infant from Set5 and Figure 6 shows a lady from Set5 both scaled by a ratio of 4. Obviously, our ANNet is able to retrieve more information from images. These findings show that our suggested ANNet is an effective single-image SR technique.

6 Conclusions

In this article, we investigate two underexplored challenges in single-image super-resolution using deep neural networks:
One of them is how to factor in image-preceding context when methods based on deep learning, and the other is how to keep the cell from adapting to various picture elements. The weights of a projection matrix learned under a tight picture previous restriction are transferred to a single convolution layer using transfer learning technology, solving the first issue. To address the second issue, the suggested ANNet maps each input feature vector to the high-resolution space using the appropriate convolution layer and attaches it to an atom in the dictionary. We suggest an embedded neighborhood deep network for single-image super-resolution that addresses these two issues. Compared to other state-of-the-art single-image super resolution techniques, our suggested strategy works better in experiments. The more data we feed into our network, the better it performs, as shown by our tests. To further enhance the network's efficiency, we are motivated to train it on a bigger dataset, such as Image Net, in preparation for real-world use.

References

1. M Bevilacqua, A Roumy, C Guillemot, ML Alberi-Morel, Low-complexity single-image super-resolution based on nonnegative neighbor embedding. (British Machine Vision Association, BMVA, 2012). https://www. engineeringvillage.com/search/doc/detailed.url?SEARCHID=caf6296bM0b6eM48c7M8336Mbde1f8cff1a7&usageZone=resultslist&usageOrigin=searchresults&pageType=quickSearch&searchtype=quickSearch&CID=quickSearchDetailedFormat&DOCINDEX=1&database=1&format=quickSearchDetailedFormat&tagscope=&displayPagination=yes
2. J Caballero, C Ledig, A Aitken, A Acosta, J Totz, Z Wang, W Shi, inProceedings of the 30th IEEE Conference on Computer Vision and PatternRecognition, CVPR. Real-time video super-resolution with spatio-temporalnetworks and motion compensation, (2017), pp. 2848–2857 https://www.engineeringvillage.com/search/doc/detailed.url?SEARCHID=ffefb3e7Mb3c2M44e8Ma22eM42bbf72807b0&usageZone=resultslist&usageOrigin=searchresults&pageType=quickSearch&searchtype=quickSearch&CID= quickSearchDetailedFormat&DOCINDEX=1&datab

ase=1&format=quickSearchDetailedFormat&tagscope=&displayPagination=yes

3. H Chang, DY Yeung, Y Xiong, in Computer Vision and Pattern Recognition,2004. CVPR 2004. Proceedings of the 2004 IEEE Computer Society Conferenceon, vol. 1. Super-resolution through neighbor embedding (Institute of Electrical and Electronics Engineers Computer Society, 2004), pp. I–I. https://www.engineeringvillage.com/search/doc/detailed.url?SEARCHID=32a31d81M1dbcM4166M9621Mc35ebfa5d73f&usageZone=resultslist&usageOrigin=searchresults&pageType=quickSearch&searchtype=quickSearch&CID=quickSearchDetailedFormat&DOCINDEX=5&database=1&format=quickSearchDetailedFormat&tagscope=&displayPagination=yes

*4. BW Chen, X He, SY Kung, Support vector analysis of large-scale databased on kernels with iteratively increasing order. J. Supercomput. **72**(9),3297–3311 (2015)*

*5. BW Chen, M Imran, M Guizani, Cognitive sensors based on ridgephase-smoothing localization and multiregional histograms of orientedgradients. IEEE Trans. Emerg. Top. Comput. **99**(1), 1–1 (2016)*

*6. BW Chen, W Ji, Geo-conquesting based on graph analysis forcrowdsourced metatrails from mobile sensing. IEEE Commun. Mag. **55**(1),92–97 (2017)*